

# Polymer Chemistry

Accepted Manuscript



This is an *Accepted Manuscript*, which has been through the Royal Society of Chemistry peer review process and has been accepted for publication.

*Accepted Manuscripts* are published online shortly after acceptance, before technical editing, formatting and proof reading. Using this free service, authors can make their results available to the community, in citable form, before we publish the edited article. We will replace this *Accepted Manuscript* with the edited and formatted *Advance Article* as soon as it is available.

You can find more information about *Accepted Manuscripts* in the [Information for Authors](#).

Please note that technical editing may introduce minor changes to the text and/or graphics, which may alter content. The journal's standard [Terms & Conditions](#) and the [Ethical guidelines](#) still apply. In no event shall the Royal Society of Chemistry be held responsible for any errors or omissions in this *Accepted Manuscript* or any consequences arising from the use of any information it contains.

**Synthesis and Phase Behavior of a New 2-Vinylbiphenyl-Based  
Mesogen-Jacketed Liquid Crystalline Polymer with High Glass Transition  
Temperature and Low Threshold Molecular Weight**

Qi-Kai Zhang,<sup>1</sup> Hai-Jian Tian,<sup>1</sup> Chang-Feng Li,<sup>1,2</sup> Yu-Feng Zhu,<sup>1</sup> Yongri Liang,<sup>3</sup> Zhihao Shen,<sup>1,\*</sup>  
and Xing-He Fan<sup>1,\*</sup>

<sup>1</sup> *Beijing National Laboratory for Molecular Sciences, Department of Polymer Science and Engineering, and Key Laboratory of Polymer Chemistry and Physics of Ministry of Education, College of Chemistry and Molecular Engineering, Peking University, Beijing 100871, China*

<sup>2</sup> *School of Materials Science and Engineering, Beijing Institute of Technology, Beijing 100081, China*

<sup>3</sup> *State Key Laboratory of Polymer Physics and Chemistry, Joint Laboratory of Polymer Science and Materials, Beijing National Laboratory for Molecular Sciences, and Institute of Chemistry, Chinese Academy of Science, Beijing 100190, China*

\* To whom the correspondence should be addressed. E-mail: fanxh@pku.edu.cn (X.-H.F.); zshen@pku.edu.cn (Z.S.).

**ABSTRACT:** We have synthesized a new mesogen-jacketed liquid crystalline polymer, poly(4'-(methoxy)-2-vinylbiphenyl-4-methyl ether) (PMVBP) containing a biphenyl core in the side-chain. PMVBP has a smaller monomer molecular weight (MW), a higher glass transition temperature, and a lower threshold MW for liquid crystalline (LC) formation. PMVBPs were obtained by nitroxide-mediated polymerization and characterized by gel permeation chromatography, differential scanning calorimetry, polarized light microscopy, and one- and two-dimensional wide-angle X-ray diffraction (WAXD) experiments. The number-average MWs ( $M_n$ 's) of these polymers range from  $0.41 \times 10^4$  to  $1.64 \times 10^4$  g/mol. A relatively high glass transition temperature is observed, which increases from 173 to 208 °C with increasing MW. The LC phase developed at relatively high temperatures is strongly dependent on the  $M_n$  of the polymer. A hexagonal columnar ( $\Phi_H$ ) LC phase is observed above 260 °C when the  $M_n$  is only above  $0.53 \times 10^4$  g/mol, a low threshold MW for LC formation. All the LC phases retain during cooling.

## INTRODUCTION

As one of the most widely used functional materials of soft matter, liquid crystalline polymers (LCPs) have received much attention owing to their various supramolecular self-assembled structures and phase transitions<sup>1-5</sup> as well as their remarkable applications in organic semiconducting materials, nonlinear optical devices, engineering plastics, self-assembled nanomaterials, and so on.<sup>6-9</sup> Mesogen-jacketed liquid crystalline polymers (MJLCPs), first

reported by Zhou et al. in 1987, have bulky side groups laterally attached to the main chain through a carbon-carbon bond or a very short spacer, and they can act as supramolecular mesogens to form liquid crystalline (LC) phases.<sup>10-12</sup> In the past few decades, many MJLCPs have been designed with novel structures and potential applications as electroluminescent materials,<sup>13-17</sup> birefringent films for optical compensators,<sup>18</sup> surface-modifying agents,<sup>19</sup> and so on. MJLCPs with side-chain cores based on 2-vinylhydroquinone,<sup>11</sup> 2-vinyl-1,4-phenylenediamine,<sup>20</sup> 2-vinylterephthalic acid,<sup>21-23</sup> vinyl terphenyl,<sup>24,25</sup> and vinyl biphenyl<sup>26-29</sup> have been synthesized. Various LC phases are obtained, such as hexagonal columnar ( $\Phi_H$ ) phase,<sup>30-32</sup> columnar nematic ( $\Phi_N$ ) phase,<sup>22,28</sup> hexatic columnar nematic ( $\Phi_{HN}$ ) phase,<sup>22,23</sup> rectangular columnar ( $\Phi_R$ ) phase,<sup>33</sup> and smectic A ( $S_mA$ ) and smectic C ( $S_mC$ ) phases.<sup>14,26,34</sup>

However, in our previous studies, control of the threshold molecular weight (MW) for the formation of LC phases and the glass transition temperature ( $T_g$ ) has not been a focus. High  $T_g$ 's and LC states can improve the service conditions and maintain the physical network of thermoplastic elastomers. Due to the difficulty in obtaining high MWs of the coil segments in thermoplastic elastomers, design and synthesis of an MJLCP with a smaller MW of the monomer, a higher glass transition temperature, and a lower threshold MW for LC formation are crucial to obtain high-performance thermoplastic elastomers based on MJLCPs.

The MW of the monomer is determined by its chemical structure, and the  $T_g$  and the threshold MW for LC formation of an MJLCP are dramatically influenced by the chemical

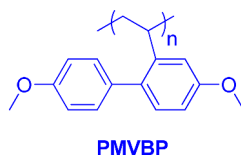
structure of the monomer and the degree of polymerization.<sup>22,35</sup> For MJLCPs with 2-vinylterephthalic acid in the side-chain core, the typical poly{2,5-bis[(4-methoxyphenyl)oxycarbonyl]styrenes} (PMPCS), with a monomer (MPCS) MW of 404 g/mol, has a  $T_g$  of about 120 °C, and it becomes liquid crystalline only when the number-average MW ( $M_n$ ) is above  $10^4$  g/mol. In between  $1.0 \times 10^4$  and  $1.6 \times 10^4$  g/mol, a  $\Phi_N$  phase forms. Above  $1.6 \times 10^4$  g/mol, a  $\Phi_{HN}$  phase is observed.<sup>22</sup> However, poly{2,5-bis[(4-butoxyphenyl)oxycarbonyl]styrenes} (PBPCS), with a monomer (BPCS) MW of 488 g/mol, has a  $T_g$  of about 108 °C because of the longer alkoxy tail. When the  $M_n$  is over  $3.4 \times 10^4$  g/mol, PBPCS forms an LC phase at high temperatures.<sup>23</sup>

For MJLCPs with vinyl terphenyl in the side-chain core, poly[2,5-bis(4'-alkoxyphenyl)styrenes] have been synthesized to investigate the influence of the alkoxy tail length on the LC behaviors of the polymers.<sup>24</sup> Among these samples, when the alkoxy tail is methoxyl group, with a monomer MW of 316 g/mol, the  $T_g$  is 230 °C, and the threshold MW for LC formation is  $3.1 \times 10^4$  g/mol. For MJLCPs with vinyl biphenyl in the center of the side-chain core, 4,4'-bis(4-butoxyphenyloxycarbonyl)-2-vinylbiphenyl (PBP2VBP) and 4,4'-bis(4-butoxyphenyloxycarbonyl)-3-vinylbiphenyl (PBP3VBP), with a monomer MW of 564 g/mol, have  $T_g$ 's of 104 and 110 °C, respectively,<sup>26</sup> possibly caused by the flexible ester linkages in the side chains. The threshold MWs of the polymers for LC formation are  $2.4 \times 10^4$  g/mol.

In this work, we aimed to design and synthesize an MJLCP with a smaller monomer MW, a higher  $T_g$ , and a lower threshold MW for LC formation. For the three systems mentioned above,

the  $T_g$  increases with increasing conjugacy and rigidity in the side-chain mesogen of the polymer when the same flexible alkyl substituent is used, while the threshold MW for LC formation increases with increasing aspect ratio of the polymer. Therefore, we should design the monomer with high rigidity, a small MW, and a small diameter. Vinyl terphenyl is not a suitable side-chain core to use because it has a higher monomer MW and a larger column diameter which tend to increase the threshold MW of the polymer. As a result, we synthesized an MJLCP containing a 2-vinylbiphenyl core in the side chains. In order to obtain a higher  $T_g$ , we chose methoxy as the flexible substituent at the side-chain ends. The structure of the designed polymer, poly[4'-(methoxy)-2-vinylbiphenyl-4-methyl ether] (PMVBP), is shown in Chart 1. The dependence of LC properties on the MW of PMVBP is also investigated.

**Chart 1.** Chemical structure of PMVBP



## EXPERIMENTAL SECTION

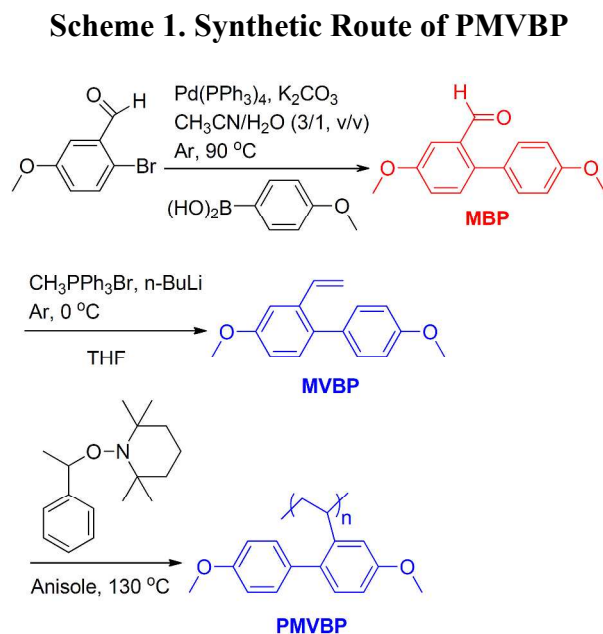
**Materials.** 2-Bromo-5-methoxybenzaldehyde (Sigma-Aldrich, 97%), 4-methoxyphenylboronic acid (J&K, 98%), tetrakis(triphenylphosphine)palladium(0) ( $\text{Pd}(\text{PPh}_3)_4$ , Sigma-Aldrich, 99%), methyltriphenylphosphonium bromide (Sigma-Aldrich, 98%), and *n*-butyllithium (J&K, 2.4 M solution in hexanes) were used as received without further

purification. Anisole (Beijing Chemical Reagents Co., A.R.) was washed with NaOH and distilled water and then distilled from calcium hydride. Tetrahydrofuran (THF, Beijing Chemical Reagents Co., A.R.) was refluxed over sodium and distilled before use. All other reagents were commercially available and used as received.

**Measurements.** The chemical structures of the intermediates and the monomer were characterized by  $^1\text{H}/^{13}\text{C}$  NMR, high resolution mass spectroscopy (HR-MS), and elemental analysis (EA).  $^1\text{H}$  NMR (400 MHz) and  $^{13}\text{C}$  NMR (100 MHz) spectra were obtained with a Bruker ARX400 spectrometer using deuterated chloroform as the solvent and tetramethylsilane as the internal standard at ambient temperature. HR-MS were recorded on a Bruker Apex IV Fourier-transform ion cyclotron resonance mass spectrometer by electrospray ionization (ESI). EA was carried out with an Elementar Vario EL instrument. Other characterization methods, such as gel permeation chromatographic (GPC) measurements, thermogravimetric analysis (TGA), differential scanning calorimetry (DSC), polarized light microscopy (PLM), and one-dimensional wide-angle X-ray diffraction (1D WAXD) experiments, were performed according to the procedures previously described.<sup>32,36</sup> Two-dimensional (2D) WAXD measurements were performed on a Rigaku S/MAX 3000 with MicroMax-007HF system equipped with a Cu ( $\lambda = 1.54 \text{ \AA}$ ) rotating anode operated at 40 kV and 30 mA and an imaging plate detector (size: 150 mm  $\times$  150 mm, Fuji Co.). The 2D WAXD data were calibrated by silicon powder ( $2\theta = 28.44^\circ$  @ 1.54  $\text{\AA}$  of wavelength).

**Synthesis of the PMVBP Polymers.** The synthetic route of PMVBP is shown in Scheme 1.

The experimental details are described in the supporting information.



## RESULTS AND DISCUSSION

**Synthesis and Characterization of Monomer and Polymers.** As shown in Scheme 1, the monomer containing a biphenyl core in the side chains could be successfully prepared in two efficient steps. 4,4'-bis(methoxy)biphenyl-2-carbaldehyde (MBP) was synthesized by a Suzuki cross-coupling reaction with 2-bromo-5-methoxybenzaldehyde and 4-(methoxy)phenylboronic acid in a high yield (91%). Then the monomer MVBP was efficiently obtained by a typical Wittig reaction.



In an alternative route, we can firstly synthesize the precursor 2-bromo-5-methoxy-1-vinylbenzene by a Wittig reaction, followed by a Suzuki cross-coupling reaction, to obtain the target monomer. In consideration of high reaction temperature for the Suzuki cross-coupling reaction, the intermediates or the monomer can possibly undergo thermal polymerization at such high temperatures. Therefore, the synthetic route as shown in Scheme 1 was chosen. The chemical structures of the intermediates and the monomer were confirmed by  $^1\text{H}$  NMR,  $^{13}\text{C}$  NMR, HR-MS, and EA.

Nitroxide-mediated living radical polymerization (NMP) is a controlled/living radical polymerization (CLRP) method that is applicable to obtain well-defined functional polymers.<sup>37,38</sup> A series of PMVBPs with different  $M_n$ 's and relatively low polydispersity indexes (PDIs) were synthesized by NMP in anisole (as shown in Scheme 1). Figures 1 and S3 (in supporting information) give the  $^1\text{H}$  and  $^{13}\text{C}$  NMR spectra of the monomer MVBP, respectively. The  $^1\text{H}$  NMR spectrum of the corresponding polymer PMVBP in  $\text{CDCl}_3$  is also shown in Figure 1, with the characteristic resonances of the vinyl group in the monomer appearing at  $\delta = 5.17\text{--}5.20$ ,  $5.65\text{--}5.70$ , and  $6.67\text{--}6.74$  ppm. After polymerization, the signals of the vinyl group completely disappear, and the resonance peaks of PMVBP are rather broad owing to slower motion of the protons, indicating the successful polymerization. The polymers are quite soluble in common organic solvents, such as anisole, chloroform, dichloromethane, chlorobenzene, THF, and so on.

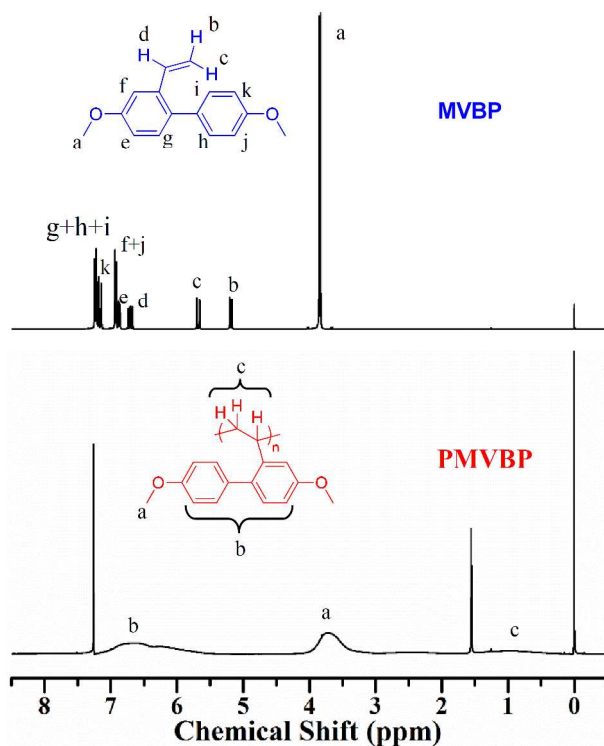


**Figure 1.** <sup>1</sup>H NMR spectra of the monomer MVBP (the top line) and the corresponding polymer PMVBP with  $M_n = 1.11 \times 10^4$  g/mol (the bottom line).

The characterization results of the polymers are summarized in Table 1. A variety of samples were synthesized by changing the ratio of initiator to monomer. GPC analysis (as shown in Figure 2) of PMVBPs shows that no monomer exists in the polymer samples, and the  $M_n$  values of the polymers range from  $0.41 \times 10^4$  to  $1.64 \times 10^4$  g/mol, with relatively low PDIs ( $< 1.4$ ), which demonstrates good controllability of the NMP process.

**Table 1. Characteristics and Thermal Properties of PMVBPs**

sample	$M_n$ ( $\times 10^4$ g/mol) <sup>a</sup>	PDI <sup>a</sup>	$T_d$ ( $^{\circ}\text{C}$ ) <sup>b</sup>	$T_g$ ( $^{\circ}\text{C}$ ) <sup>c</sup>	Liquid Crystallinity <sup>d</sup>
PMVBP-1	0.41	1.36	367	173	No
PMVBP-2	0.53	1.37	365	185	Yes
PMVBP-3	0.86	1.33	376	191	Yes
PMVBP-4	1.11	1.29	369	207	Yes
PMVBP-5	1.64	1.31	375	208	Yes

<sup>a</sup>  $M_n$  and PDI values of the polymers determined by GPC in THF using PS standards.

<sup>b</sup> The temperatures at 5% weight loss of the polymers evaluated by TGA heating experiments under a nitrogen atmosphere at a heating rate of 20  $^{\circ}\text{C}/\text{min}$ .

<sup>c</sup> The glass transition temperatures of the polymers measured under a nitrogen atmosphere by DSC at a scanning rate of 20  $^{\circ}\text{C}/\text{min}$  during the second heating cycle.

<sup>d</sup> Evaluated by PLM and 1D WAXD measurements.

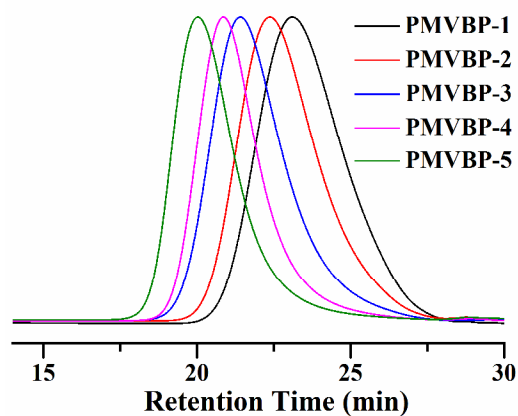


**Figure 2.** GPC curves of PMVBPs.

**Thermal Properties and Phase Behaviors of the Polymers.** The thermal properties of the polymers were characterized by TGA. The thermogravimetric curves are shown in Figure S4 of supporting information. As shown in Table 1 and Figure S4, all polymers exhibit excellent thermal stabilities under the nitrogen atmosphere, and their 5% weight loss temperatures ( $T_d$ 's) are all about 370 °C.

The phase transitions of the polymers were characterized by DSC experiments. All samples were heated from ambient temperature to 280 °C at a rate of 20 °C/min in order to eliminate thermal history. Then the PMVBP polymers were cooled at a rate of 10 °C/min and heated at a rate of 20 °C/min under the nitrogen atmosphere. All the DSC thermograms only exhibit glass transitions (as shown in Figure 3), similar to many other MJLCPs reported previously.<sup>22,23,28,32,39</sup> The second heating processes were used to obtain the  $T_g$  values, with the results listed in Table 1. Common for polymers including PMPCS, a typical MJLCP, the  $T_g$  value of PMVBP also shows an MW dependence.<sup>22,35</sup> PMVBP exhibits a relatively high  $T_g$  (173 °C) even at a relatively low  $M_n$  of  $0.41 \times 10^4$  g/mol.  $T_g$  increases with increasing  $M_n$  and levels off at about 210 °C when the  $M_n$  increases to  $1.11 \times 10^4$  g/mol. The  $T_g$  value of PMVBP is much higher than those of most other MJLCPs, such as PMPCS (about 120 °C),<sup>22</sup> PBPCS (about 108 °C),<sup>23</sup> and so on,<sup>27,40</sup> probably owing to the lack of flexible linkages such as ester connections in the side chain.

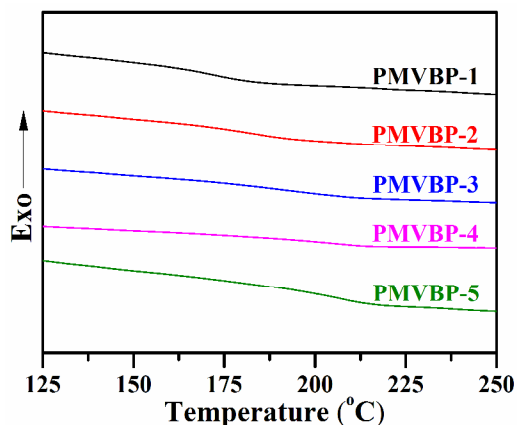


**Figure 3.** DSC thermograms of PMVBPs during the second heating at a rate of 20 °C/min under the nitrogen atmosphere.  $T_g$  increases with increasing  $M_n$ .

**Liquid Crystalline Properties and Phase Structures of the Polymers.** The monomer and the polymers were all white solids at ambient temperature. No liquid crystallinity of the monomer during PLM experiments was observed at different temperatures. Polymer samples were cast from THF solutions and slowly dried at ambient temperature. Some polymers, such as PMVBP-1, PMVBP-3, and PMVBP-5, showed very weak birefringence at ambient temperature, possibly caused by orientation of the polymer chains during precipitation. However, such results can not illustrate whether the polymers are liquid crystalline. Upon heating, the polymers showed different properties depending on the MWs. The sample PMVBP-1 with an  $M_n$  of  $0.41 \times 10^4$  g/mol did not show a large area of birefringence during heating up to 280 °C. However, PMVBP-2 with an  $M_n$  of  $0.53 \times 10^4$  g/mol clearly exhibited birefringence during heating up to 240 °C. A schlieren-like texture was observed during further heating at 250 °C (as shown in

Figure 4a). The birefringence of PMVBP-2 remained when it was cooled to ambient temperature. Analogously, as shown in Figure 4b, PMVBP-3 also showed a schlieren-like texture when it was heated to 310 °C and cooled to 270 °C. With further increase in MW, the  $T_g$  of PMVBP-4 and PMVBP-5 increase to 208 °C. These two samples are very rigid, and the temperatures at which liquid crystalline phases start to develop are higher than those of other samples. Birefringence was detected at 278 and 290 °C for PMVBP-4 and PMVBP-5, respectively. However, the textures of these two samples were not typical ones, possibly due to the low mobilities of the polymer chains. Therefore, clear birefringence of all the samples except PMVBP-1 was observed, and it remained when the samples were cooled down to ambient temperature. This phenomenon is similar to that of some MJLCPs reported previously.<sup>21,26,32</sup> Specifically, PMVBP starts to show liquid crystallinity at a much lower  $M_n$  of only  $0.5 \times 10^4$  g/mol, compared with most other MJLCPs, such as PMPCS, which forms a  $\Phi_N$  phase when  $M_n$  is in between  $1.0 \times 10^4$  and  $1.6 \times 10^4$  g/mol and a  $\Phi_{HN}$  phase with  $M_n$  over  $1.6 \times 10^4$  g/mol.<sup>22</sup>

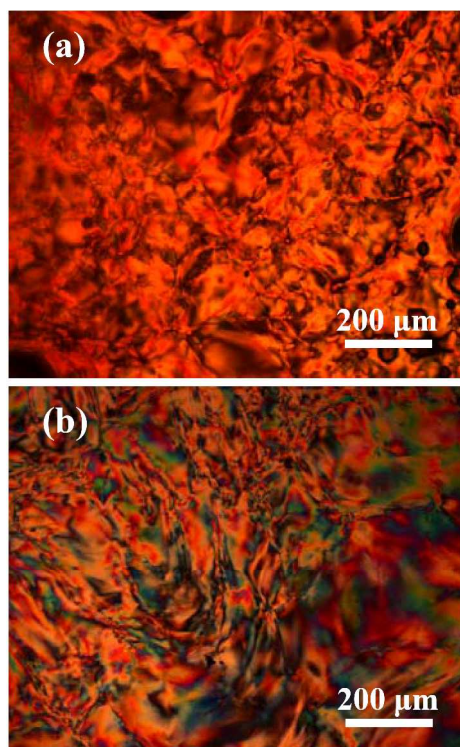


**Figure 4.** PLM micrographs of solution-cast films of PMVBP-2 taken at 250 °C (a) and PMVBP-3 at 270 °C during cooling after it was heated to 310 °C (b).

Because the textures in PLM experiment may not determine the exact phase structures, the phase behaviors of the samples were further characterized by variable-temperature 1D WAXD experiments. In these experiments, polymer samples of about 30 mg were cast from THF solutions, and then the solvents were evaporated at ambient temperature. Two sets of 1D WAXD patterns of PMVBP-1 (with an  $M_n$  of  $0.41 \times 10^4$  g/mol) recorded during the first heating and subsequent cooling processes are shown in Figure 5. At low temperatures, the profiles of the sample only demonstrate two scattering halos at a low  $2\theta$  value of  $6.75^\circ$  and a high  $2\theta$  value of  $20.11^\circ$ , respectively. The intensity of the low-angle scattering halo increases a little upon the first

heating, as shown in Figure 5a, but still remains as a broad scattering halo for the whole temperature range studied, even at 280 °C. Upon cooling, as shown in Figure 5b, the intensity of the low-angle scattering halo remains the same. Figure 5c shows the change in the  $d$ -spacing of the low-angle halo as a function of temperature during the first heating and subsequent cooling processes for PMVBP-1. The  $d$ -spacing does not show any sharp changes at temperatures above  $T_g$  during heating and cooling, indicating that no liquid crystalline phase transitions occur when temperature is changed. With the combination of PLM results, it can be concluded that PMVBP-1 with a low  $M_n$  of  $0.41 \times 10^4$  g/mol is not liquid crystalline.

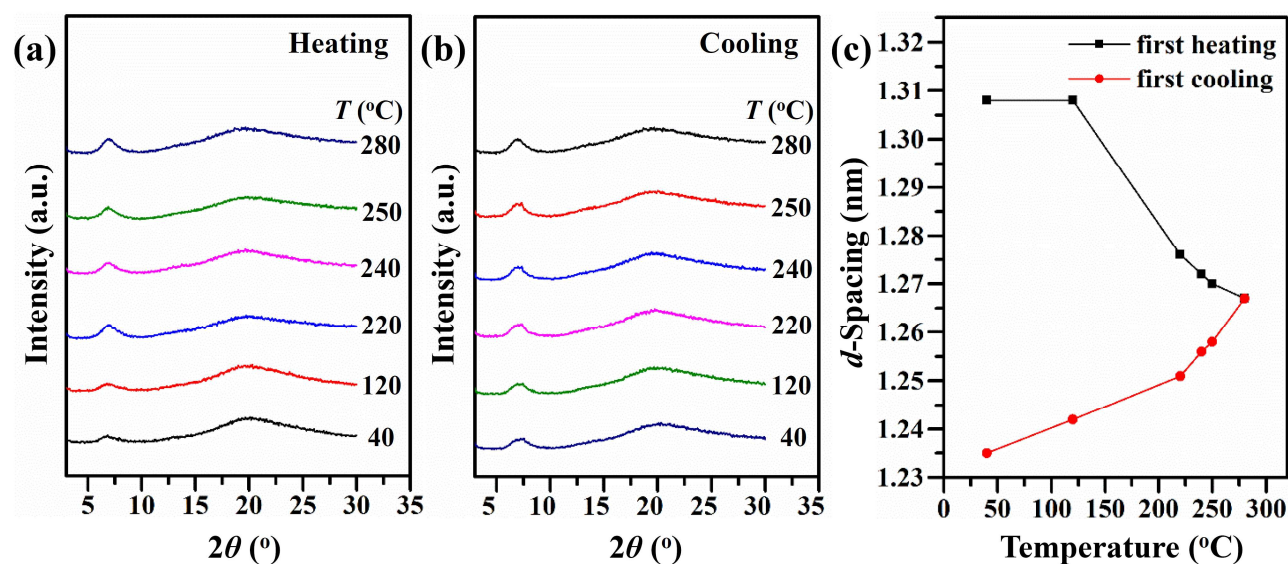


**Figure 5.** 1D WAXD patterns of PMVBP-1 during the first heating (a) and the subsequent cooling (b) processes under a nitrogen atmosphere and the  $d$ -spacing of the low-angle halo as a function of temperature (c) during the first heating and the subsequent cooling processes as shown in (a) and (b).



The phase behavior of PMVBP-2 was also examined by variable-temperature 1D WAXD experiments. Two sets of 1D WAXD patterns of PMVBP-2 (with an  $M_n$  of  $0.53 \times 10^4$  g/mol) obtained during the first heating and subsequent cooling processes are shown in parts a and b of Figure 6, respectively. At ambient temperature, the WAXD profile also shows two scattering halos at a low  $2\theta$  value of  $6.71^\circ$  and a high  $2\theta$  value of  $19.99^\circ$ , respectively. Upon the first heating (as shown in Figure 6a), a sharp diffraction peak in the low-angle region develops at  $260^\circ\text{C}$ , which is higher than the  $T_g$  of the sample. The peak slightly shifts to a higher angle of  $7.20^\circ$ . The intensity of the low-angle peak at high temperatures is much higher than that of the halo at ambient temperature and is also much higher than that of the halo from PMVBP-1 at high temperatures, which indicates the development of an ordered structure. Along with the PLM result in Figure 4a, such an ordered structure is an LC phase. No higher-order diffraction peaks of the low-angle peak are observed in the 1D WAXD experiments, while the high-angle scattering halo moves to lower angles with increasing temperature mainly due to thermal expansion. Upon cooling, as shown in Figure 6b, the intensity of the low-angle diffraction peak remains the same, indicating that the LC phase of PMVBP-2 maintains upon cooling.

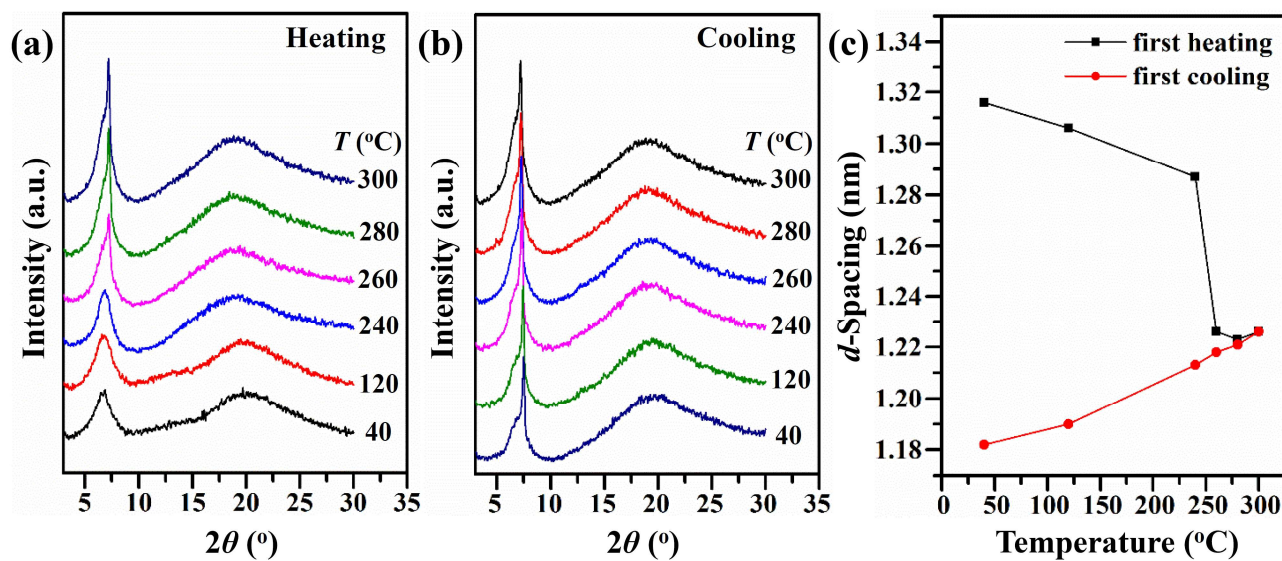


**Figure 6.** 1D WAXD patterns of PMVBP-2 during the first heating (a) and the subsequent cooling (b) processes under a nitrogen atmosphere and the  $d$ -spacing of the low-angle halo/peak as a function of temperature (c) during the first heating and the subsequent cooling processes as shown in (a) and (b).

Figure 6c summarizes the  $d$ -spacing changes of the low-angle scattering halo or diffraction peak as a function of temperature during the first heating and subsequent cooling processes for PMVBP-2. Upon the first heating, the  $d$ -spacing decreases a little with increasing temperature before 240 °C, then decreases sharply between 240 and 260 °C until it levels off (the black line). This sharp change indicates a first-order transition which is the formation of the LC phase. On the other hand, the  $d$ -spacing decreases monotonically during cooling, indicating that no phase transition occurs, and the slope of the cooling line (the red line) represents the coefficient of thermal expansion (CTE) of the structure studied.<sup>22</sup> The CTE value is about  $1.7 \times 10^{-4}$  nm/°C.

Because no higher-order diffraction peaks of the low-angle peak in the 1D WAXD experiments were observed, the sample was further treated with thermal annealing in vacuum at 260 °C for 0.5 h. As shown in Figure 7, a higher-order diffraction peak is observed after thermal annealing. The 1D WAXD profile of the sample at 260 °C demonstrates two diffraction peaks at low  $2\theta$  values of 7.35° and 12.87°. The scattering vectors ( $q_s$ ) of these two peaks are 5.23 and 9.14 nm<sup>-1</sup>, respectively, and their ratio is 1:3<sup>1/2</sup>, indicating a hexagonal packing. Therefore, PMVBP-2 has a  $\Phi_H$  structure. These two diffraction peaks remain during the cooling process, with the peaks slightly shifting to higher angles. From the  $d$ -spacing value of 1.17 nm at 40 °C, the hexagonal lattice parameter  $a$ , which is the distance between neighboring polymer rods, can be calculated as 1.35 nm. This value is nearly equal to the simulated length (1.32 nm) of the side chain of the polymer, indicating that the side chains are aligned almost perpendicular to the main chain.

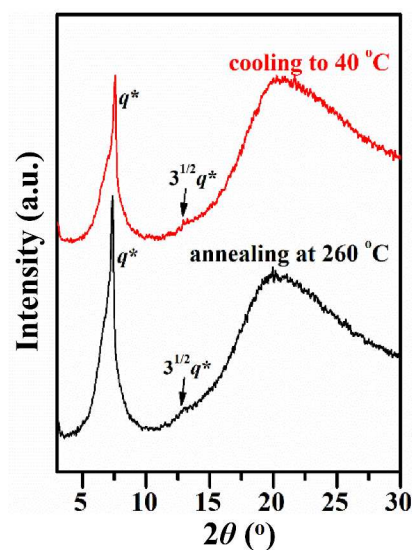


**Figure 7.** 1D WAXD patterns of PMVBP-2 after annealing at 260 °C for 0.5 h (the black line)

and the subsequent cooling (the red line) under a nitrogen atmosphere.

PMVBP-3 shows similar 1D WAXD results (Figure S5 in the supporting information) as PMVBP-2. The difference is that without thermal annealing, the WAXD profile of PMVBP-3 at 240 °C during heating shows the second-order diffraction peak of the  $\Phi_H$  phase which retains during cooling.

The results of PMVBP-4 are also similar. The 1D WAXD patterns are shown in Figure 8, with the second-order peak clearly visible, suggesting that the liquid crystalline structure is more ordered. The scattering vector ratio is also  $1:3^{1/2}$ , indicating a  $\Phi_H$  phase. The  $d$ -spacing also shows a sharp decrease during heating (Figure 8c, the black line) owing to the formation of the LC phase. The CTE value is about  $1.6 \times 10^{-4}$  nm/°C.

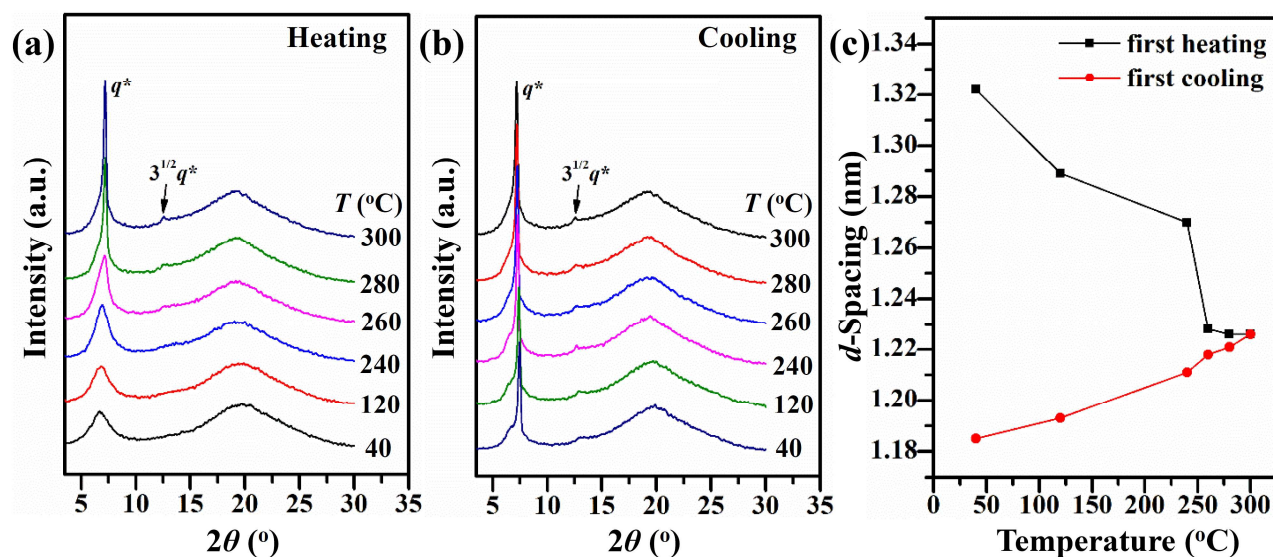


**Figure 8.** 1D WAXD patterns of PMVBP-3 during the first heating (a) and the subsequent cooling (b) processes under a nitrogen atmosphere and the  $d$ -spacing of the low-angle halo/peak

as a function of temperature (c) during the first heating and the subsequent cooling processes as shown in (a) and (b).

The 1D WAXD results of PMVBP-5 are similar to those of PMVBP-3 and PMVBP-4. The 1D WAXD patterns are shown in Figure S6 of the supporting information. A  $\Phi$ H phase is also formed during heating, and it retains upon cooling. For PMVBP-2, PMVBP-3, PMVBP-4, and PMVBP-5, the WAXD profiles at low temperatures after cooling all have a shoulder halo appearing at the left of the first-order low-angle diffraction peak. This may be caused by the amorphous phase of low-MW fractions in the polymers.

Finally, in order to further confirm the liquid crystalline phases of PMVBPs, 2D WAXD experiments were conducted with mechanically sheared samples with the consideration of the dimensionality limit of 1D WAXD experiments. Taking PMVBP-3 which was mechanically sheared at 280 °C as an example, Figure 9a shows its 2D WAXD pattern with the X-ray beam along  $Y$  direction which is perpendicular to the shear direction ( $X$  direction, the shear geometry shown in Figure 9b). Two pairs of diffraction arcs in the low-angle region on the equator can be clearly discerned, which demonstrates the existence of an ordered structure with lattice planes oriented parallel to the meridian direction which is the direction of polymer main chains upon shearing (in other words, lateral packing of the polymer chains). An additional higher-order diffraction peak appears in the 1D WAXD pattern (Figure 9c) obtained through integration of the 2D pattern. The scattering vector ratio of the peaks is  $1:3^{1/2}:2$ , confirming a  $\Phi$ <sub>H</sub> structure, and the

peaks can be assigned as (100), (110), and (200) diffractions.

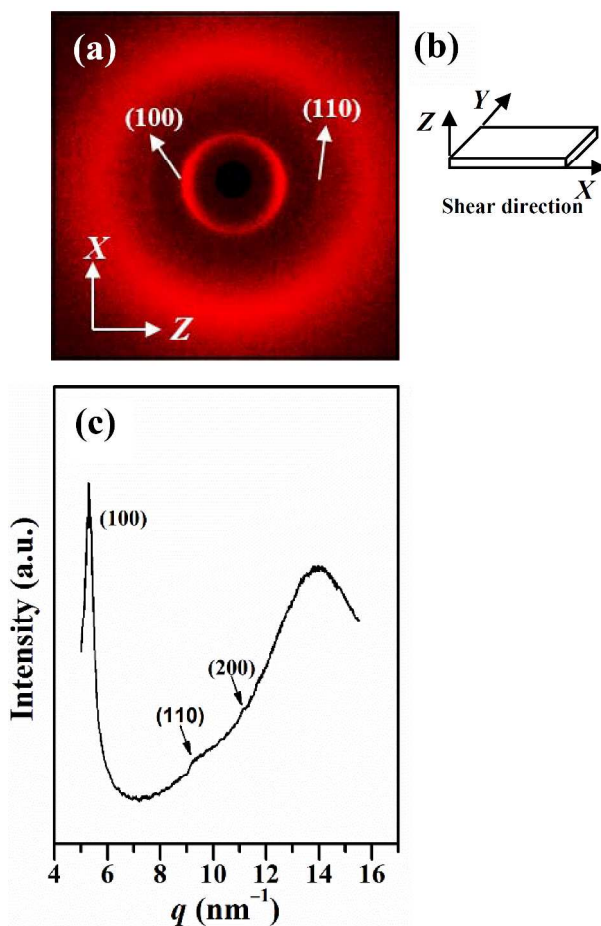


**Figure 9.** 2D WAXD pattern of PMVBP-3 at ambient temperature with the X-ray beam perpendicular to the shear direction (a), the shearing geometry (b) with  $X$  direction as the shear direction, and the integral 1D WAXD pattern (c) obtained from (a).

The phase behavior of PMVBP with increasing MW can be summarized in the phase diagram shown in Figure 10. PMVBP can form a liquid crystalline phase at relatively low MWs, compared to other MJLCPs. When the  $M_n$  is higher than  $0.53 \times 10^4$  g/mol, it can develop into a

$\Phi_H$  LC phase above 250 °C upon the first heating, and the LC phase remains during cooling.

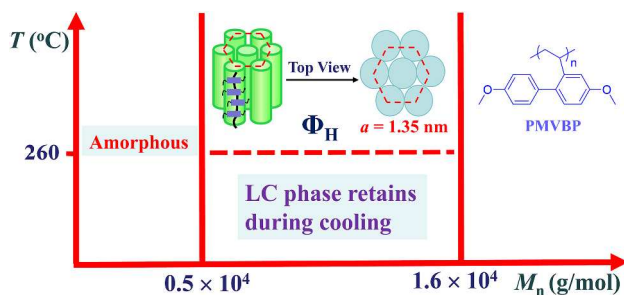


**Figure 10.** Schematic drawing of the phase diagram for PMVBPs.

## CONCLUSIONS

In summary, we have obtained a new series of MJLCP, PMVBPs, based on a 2-vinylbiphenyl monomer with a smaller monomer MW, a higher glass transition temperature, and a lower threshold MW for LC formation. PMVBPs with different  $M_n$ 's and relatively low PDIs were synthesized by NMP. The  $M_n$ 's of these polymers determined by GPC are in the range of  $0.41 \times 10^4$  to  $1.64 \times 10^4$  g/mol.  $T_g$  increases with increasing  $M_n$  and levels off at about 210 °C. And the  $T_g$  value of PMVBP is higher than those of most other MJLCPs. PMVBP can form a  $\Phi_H$  phase at relatively low MWs, compared to other MJLCPs. When the  $M_n$  is higher than only  $0.53 \times 10^4$  g/mol, it can develop into a  $\Phi_H$  liquid crystalline phase above 250 °C upon heating, and the LC phase is maintained during cooling. Because of its higher glass transition temperature and lower threshold MW for LC formation, PMVBP is the excellent candidate as the hard segment of ABA-type thermoplastic LC elastomers. To this end, research work is currently in progress.

## ASSOCIATED CONTENT

**Supporting Information.** Synthesis of monomer and polymers, NMR spectra of the initiator and MBP, TGA curves of PMVBPs, 1D WAXD patterns of PMVBP-3 and PMVBP-5.

**Acknowledgments.** This work was supported by the National Natural Science Foundation of China (Grants 21134001 and 20990232) and the National Basic Research Program of China (973 Program, Project 2011CB606004).

## REFERENCES

- (1) Akagi, K. *J. Polym. Sci. Part A: Polym. Chem.* **2009**, *47*, 2463-2485.
- (2) Yang, S. H.; Hsu, C. S. *J. Polym. Sci. Part A: Polym. Chem.* **2009**, *47*, 2713-2733.
- (3) Hammond, M. R.; Mezzenga, R. *Soft Matter* **2008**, *4*, 952-961.
- (4) Hsu, C. S. *Prog. Polym. Sci.* **1997**, *22*, 829-871.
- (5) Tsukruk, V. V.; Bliznyuk, V. N. *Prog. Polym. Sci.* **1997**, *22*, 1089-1132.
- (6) Pisula, W.; Zorn, M.; Chang, J. Y.; Mullen, K.; Zentel, R. *Macromol. Rapid Comm.* **2009**, *30*, 1179-1202.
- (7) Funahashi, M. *Polym. J.* **2009**, *41*, 459-469.
- (8) O'Neill, M.; Kelly, S. M. *Adv. Mater.* **2011**, *23*, 566-584.
- (9) Shibaev, V.; Bobrovsky, A.; Boiko, N. *Prog. Polym. Sci.* **2003**, *28*, 729-836.
- (10) Zhou, Q. F.; Li, H. M.; Feng, X. D. *Macromolecules* **1987**, *20*, 233-234.



- (11) Zhou, Q. F.; Zhu, X. L.; Wen, Z. Q. *Macromolecules* **1989**, *22*, 491-493.
- (12) Chen, X. F.; Shen, Z. H.; Wan, X. H.; Fan, X. H.; Chen, E. Q.; Ma, Y. G.; Zhou, Q. F. *Chem. Soc. Rev.* **2010**, *39*, 3072-3101.
- (13) Gao, L. C.; Shen, Z. H.; Fan, X. H.; Zhou, Q. F. *Polym. Chem.* **2012**, *3*, 1947-1957.
- (14) Chai, C. P.; Zhu, X. Q.; Wang, P.; Ren, M. Q.; Chen, X. F.; Xu, Y. D.; Fan, X. H.; Ye, C.; Chen, E. Q.; Zhou, Q. F. *Macromolecules* **2007**, *40*, 9361-9370.
- (15) Wang, P.; Chuai, Y. T.; Chai, C. P.; Wang, F. Z.; Zhang, G. L.; Ge, G. P.; Fan, X. H.; Guo, H. Q.; Zou, D. C.; Zhou, Q. F. *Polymer* **2008**, *49*, 455-460.
- (16) Yang, Q.; Xu, Y. D.; Jin, H.; Shen, Z. H.; Chen, X. F.; Zou, D. C.; Fan, X. H.; Zhou, Q. F. *J. Polym. Sci. Part A: Polym. Chem.* **2010**, *48*, 1502-1515.
- (17) Jin, H.; Xu, Y. D.; Shen, Z. H.; Zou, D. C.; Wang, D.; Zhang, N.; Fan, X. H.; Zhou, Q. F. *Macromolecules* **2010**, *43*, 8468-8478.
- (18) Chen, S.; Zhang, L. Y.; Guan, X. L.; Fan, X. H.; Shen, Z. H.; Chen, X. F.; Zhou, Q. F. *Polym. Chem.* **2010**, *1*, 430-433.
- (19) Gopalan, P.; Andruzzi, L.; Li, X. F.; Ober, C. K. *Macromol. Chem. Phys.* **2002**, *203*, 1573-1583.
- (20) Zhang, D.; Zhou, Q. F.; Ma, Y. G.; Wan, X. H.; Feng, X. D. *Polym. Advan. Technol.* **1997**, *8*, 227-233.
- (21) Zhang, D.; Liu, Y. X.; Wan, X. H.; Zhou, Q. F. *Macromolecules* **1999**, *32*, 5183-5185.
- (22) Ye, C.; Zhang, H. L.; Huang, Y.; Chen, E. Q.; Lu, Y. L.; Shen, D. Y.; Wan, X. H.; Shen, Z. H.; Cheng, S. Z. D.; Zhou, Q. F. *Macromolecules* **2004**, *37*, 7188-7196.
- (23) Zhao, Y. F.; Fan, X. H.; Wan, X. H.; Chen, X. F.; Yi, Y.; Wang, L. S.; Dong, X.; Zhou, Q. F. *Macromolecules* **2006**, *39*, 948-956.

- (24) Yu, Z. N.; Tu, H. L.; Wan, X. H.; Chen, X. F.; Zhou, Q. F. *J. Polym. Sci. Part A: Polym. Chem.* **2003**, *41*, 1454-1464.
- (25) Zhu, Z. G.; Zhi, J. G.; Liu, A. H.; Cui, J. X.; Tang, H.; Qiao, W. Q.; Wan, X. H.; Zhou, Q. F. *J. Polym. Sci. Part A: Polym. Chem.* **2007**, *45*, 830-847.
- (26) Chen, S.; Gao, L. C.; Zhao, X. D.; Chen, X. F.; Fan, X. H.; Xie, P. Y.; Zhou, Q. F. *Macromolecules* **2007**, *40*, 5718-5725.
- (27) Chen, S.; Zhang, L. Y.; Gao, L. C.; Chen, X. F.; Fan, X. H.; Shen, Z.; Zhou, Q. F. *J. Polym. Sci. Part A: Polym. Chem.* **2009**, *47*, 505-514.
- (28) Zhang, L. Y.; Wu, H. L.; Shen, Z. H.; Fan, X. H.; Zhou, Q. F. *J. Polym. Sci. Part A: Polym. Chem.* **2011**, *49*, 3207-3217.
- (29) Zhang, L. Y.; Zhang, Y. F. *J. Polym. Sci. Part A: Polym. Chem.* **2013**, *51*, 2545-2554.
- (30) Tu, H. L.; Wan, X. H.; Liu, Y. X.; Chen, X. F.; Zhang, D.; Zhou, Q. F.; Shen, Z. H.; Ge, J. J.; Jin, S.; Cheng, S. Z. D. *Macromolecules* **2000**, *33*, 6315-6320.
- (31) Yin, X. Y.; Ye, C.; Ma, X.; Chen, E. Q.; Qi, X. Y.; Duan, X. F.; Wan, X. H.; Cheng, S. Z. D.; Zhou, Q. F. *J. Am. Chem. Soc.* **2003**, *125*, 6854-6855.
- (32) Xu, Y. D.; Yang, Q.; Shen, Z. H.; Chen, X. F.; Fan, X. H.; Zhou, Q. F. *Macromolecules* **2009**, *42*, 2542-2550.
- (33) Chen, X. F.; Tenneti, K. K.; Li, C. Y.; Bai, Y. W.; Zhou, R.; Wan, X. H.; Fan, X. H.; Zhou, Q. F. *Macromolecules* **2006**, *39*, 517-527.
- (34) Xu, Y. D.; Qu, W.; Yang, Q.; Zheng, J. K.; Shen, Z. H.; Fan, X. H.; Zhou, Q. F. *Macromolecules* **2012**, *45*, 2682-2689.
- (35) Zhang, H.; Yu, Z.; Wan, X.; Zhou, Q. F.; Woo, E. M. *Polymer* **2002**, *43*, 2357-2361.

- (36) Zhang, L. Y.; Chen, S.; Zhao, H.; Shen, Z. H.; Chen, X. F.; Fan, X. H.; Zhou, Q. F. *Macromolecules* **2010**, *43*, 6024-6032.
- (37) Hawker, C. J.; Bosman, A. W.; Harth, E. *Chem. Rev.* **2001**, *101*, 3661-3688.
- (38) Nicolas, J.; Guillaneuf, Y.; Lefay, C.; Bertin, D.; Gigmes, D.; Charleux, B. *Prog. Polym. Sci.* **2013**, *38*, 63-235.
- (39) Tang, H.; Zhu, Z. G.; Wan, X. H.; Chen, X. F.; Zhou, Q. F. *Macromolecules* **2006**, *39*, 6887-6897.
- (40) Chen, S.; Luo, H. B.; Xie, H. L.; Zhang, H. L. *J. Polym. Sci. Part A: Polym. Chem.* **2013**, *51*, 924-935.

## TOC Graphic for

**Synthesis and Phase Behavior of a New 2-Vinylbiphenyl-Based Mesogen-Jacketed Liquid Crystalline Polymer with High Glass Transition Temperature and Low Threshold Molecular Weight**

Qi-Kai Zhang, Hai-Jian Tian, Chang-Feng Li, Yu-Feng Zhu, Yongri Liang, Zhihao Shen, \* and Xing-He Fan\*

PMVBP was synthesized by nitroxide-mediated polymerization. They have a smaller monomer molecular weight (MW), a higher glass transition temperature, and a lower threshold MW for liquid crystalline (LC) formation. The LC phase developed at relatively high temperatures is strongly dependent on the  $M_n$  of the polymer. All the LC phases retain during cooling.

